

Gluon distribution in nucleon and its application to
analysis of ep DIS, pp and AA collisions at high
energies and mid-rapidity

Распределение глюонов в нуклоне и его применение
к анализу ep глубоко неупругого рассеяния (ГНР),
 pp и AA столкновений при высоких энергиях и
центральной быстроте.

G.I. Lykasov^{a,1}, A.I. Malakhov^{a,2}, M.A. Malyshev^{b,3}, A.V. Lipatov^{a,b,4}, A.A. Zaitsev^{a,5}
Г.И. Лыкасов^{a,1}, А.И. Малахов^{a,2}, М.А. Мальшев^{b,3}, А.В. Липатов^{a,b,4}, А.А. Зайцев^{a,5}

^a Joint Institute for Nuclear Research, 141980, Dubna, Moscow region, Russia

^a Объединенный институт ядерных исследований, 141980, Дубна, Московская
обл., Россия

^b Skobeltsyn Institute of Nuclear Physics, Lomonosov Moscow State University,
119991, Moscow, Russia

^b Научно-исследовательский институт ядерной физики им. Д.В. Скобельцына
Московского государственного университета им. М.В. Ломоносова, 119991,
Москва, Россия

Дается обзор о распределении глюонов по поперечному импульсу (ППИ)
и его применении к анализу ep глубоко неупругого рассеяния (ГНР) при
энергиях HERA, жестких и мягких pp процессах при энергиях (БАК) и в
центральной области быстрот.

A review on the gluon transverse momentum dependent distribution (TMD)
and its application to the analysis of the ep DIS at the HERA energies, hard and
soft pp processes at LHC energies and mid-rapidity is presented.

Keywords: small- x physics, TMD gluon density, deep inelastic scattering,
color dipole approach, modified quark-gluon string model

¹E-mail: lykasov@jinr.ru

²E-mail: malakhov@jinr.ru

³E-mail: malyshev@theory.sinp.msu.ru

⁴E-mail: lipatov@theory.sinp.msu.ru

⁵E-mail: zaicev@jinr.ru

¹E-mail: lykasov@jinr.ru

²E-mail: malakhov@jinr.ru

³E-mail: malyshev@theory.sinp.msu.ru

⁴E-mail: lipatov@theory.sinp.msu.ru

⁵E-mail: zaicev@jinr.ru

1. Introduction

The description of any physical observables, obtained in the collider experiments at LHC, is mainly based on different factorization theorems in quantum chromodynamics (QCD). According to these theorems, hard partonic processes are separated from partonic density functions (PDF). An appropriate QCD evolution describing the PDF, as a function of the resolution scale μ^2 , is given by the Dokshitzer-Gribov-Lipatov-Altarelli-Parisi (DGLAP) equation [1]. This approach can be successfully applied usually to analyze inclusive hard processes, like deep-inelastic lepton-hadron scattering (DIS). The transverse momentum (k_T) dependent (TMD or unintegrated) parton densities $f_a(x, \mathbf{k}_T^2, \mu^2)$ (with $a = q$ or g) satisfy the the Balitsky-Fadin-Kuraev-Lipatov (BFKL) or Catani-Ciafaloni-Fiorani-Marchesini (CCFM) evolution equation [2].

2. Gluon TMD and its saturation at low Q^2

The CCFM evolution equation reads:

$$f_g(x, \mathbf{k}_T^2, \mu^2) = f_g^{(0)}(x, \mathbf{k}_T^2, \mu_0^2) \Delta_s(\mu, \mu_0) + \int \frac{dz}{z} \int \frac{dq^2}{q^2} \Theta(\mu - zq) \Delta_s(\mu, zq) \tilde{P}_{gg}(z, \mathbf{k}_T^2, q^2) f_g\left(\frac{x}{z}, \mathbf{k}'_T^2, q^2\right), \quad (1)$$

where $\mathbf{k}'_T = \mathbf{q}(1-z) + \mathbf{k}_T$, $\tilde{P}_{gg}(z, \mathbf{k}_T^2, q^2)$ is the CCFM splitting function [2], $\Delta_s(\mu, \mu_0)$ is the Sudakov form factor, see details in [2].

As it is shown in [3,4], the solution of this equation is very sensitive to the form of the initial gluon TMD $f_g^{(0)}(x, \mathbf{k}_T^2, \mu_0^2)$ at the starting renormalization scale μ_0^2 . There are a view type of it. Similar to conventional PDFs, a construction of the TMD parton distributions in a proton starts from the input densities, which are further used as an initial conditions for subsequent non-collinear QCD evolution. As it was mentioned above, usually the initial TMD gluon density at some starting scale μ_0^2 (which is of order of hadron scale) is taken in the rather general mathematical form with factorized Gauss smearing in transverse momentum \mathbf{k}_T^2 (see, for example, [5]):

$$f_g^{(0)}(x, \mathbf{k}_T^2, \mu_0^2) = a_1 x^{a_2} (1-x)^{a_3} e^{-\mathbf{k}_T^2/q_0^2}, \quad (2)$$

where all the parameters have to be extracted from the experimental data. Alternatively, a more physically motivated non-factorized expression for $f_g^{(0)}(x, \mathbf{k}_T^2, \mu_0^2)$ can be taken from the Golec-Biernat-Wüsthoff (GBW) approach [6,7] based on color dipole picture for deep inelastic scattering (DIS): Similar to conventional PDFs, a construction of the TMD parton distributions in a proton starts from the input densities, which are further used as an initial conditions for subsequent non-collinear QCD evolution. As it was mentioned above,

usually the initial TMD gluon density at some starting scale μ_0^2 (which is of order of hadron scale) is taken in the rather general mathematical form with factorized Gauss smearing in transverse momentum \mathbf{k}_T^2 (see, for example, [5]):

$$f_g^{(0)}(x, \mathbf{k}_T^2, \mu_0^2) = a_1 x^{a_2} (1-x)^{a_3} e^{-\mathbf{k}_T^2/q_0^2}, \quad (3)$$

where all the parameters have to be extracted from the experimental data. Alternatively, a more physically motivated non-factorized expression for $f_g^{(0)}(x, \mathbf{k}_T^2, \mu_0^2)$ can be taken from the Golec-Biernat-Wüsthoff (GBW) approach [6, 7] based on color dipole picture for deep inelastic scattering (DIS):

$$f_g^{(0)}(x, \mathbf{k}_T^2, \mu_0^2) = c_g R_0^2(x) \mathbf{k}_T^2 e^{-R_0^2(x) \mathbf{k}_T^2}, \quad R_0(x) = \frac{1}{Q_0} \left(\frac{x}{x_0} \right)^{\lambda/2}, \quad (4)$$

where $c_g = 3\sigma_0/(4\pi^2\alpha_s)$, $\sigma_0 = 29.12$ mb, $\alpha_s = 0.2$, $Q_0 = 1$ GeV, $x_0 = 4.1 \cdot 10^{-5}$ and $\lambda = 0.277$. In this approach, the effect of saturation of $q\bar{q}$ dipole cross section at large distance r between quark and anti-quark in the dipole is taken into account. The GBW model has been successfully applied to both inclusive and diffractive ep scattering at HERA. However, it meets some difficulties in the accurate description of several hard LHC processes. In our previous studies we have demonstrated that one could achieve a reasonably well description of the latter using the analytical expression (non-factorized with respect to x and \mathbf{k}_T^2) for initial TMD gluon density derived in the modified QGSM approach from the best description of inclusive hadron spectra in the mid-rapidity at low scales [3].

As it is suggested in [8], at very low x and Q^2 the proton structure function $F_2(x, Q^2)$ determined mainly by the TMD gluon density $f_g(x, k_T, Q^2)$ can be saturated, i.e., it does not depend on Q^2 . In [9] the partial saturation of the gluon TMD at Q^2 less than the saturation value Q_S^2 was suggested, i.e., $f_g(x, k_T, Q^2) \leq Q_S^2 \simeq \text{Constant} \times \ln(1/x)$. Further developments on the saturation effect were done in [6, 7, 10, 11]. At asymptotically low x , an equivalent description is provided by the color dipole model, [6, 7, 10, 11], where gluon saturation effects [9] (the partial saturation) important at low scales (and, of course, at low Q^2 in DIS) can be consistently taken into account. In this approach, the DIS events are considered as an interaction of the virtual photon decaying into a color dipole $q\bar{q}$ and a proton. The saturation of the photon-proton cross section $\sigma^{\gamma^*p}(x, Q^2)$ as a function of the transverse distance r between q and \bar{q} is suggested at large r or small Q^2 (see [6, 7] for more information). Within the dipole approach, a satisfactory description of early HERA data on the proton structure function $F_2(x, Q^2)$ and $\sigma^{\gamma^*p}(x, Q^2)$ at low x was obtained [6, 7].

The new starting gluon TMD at low Q^2 was obtained recently in [3]. It reads:

$$f_g(x, \mathbf{k}_T^2) = c_g (1-x)^{b_g} \sum_{n=1}^3 (c_n R_0(x) |\mathbf{k}_T|)^n e^{-R_0(x) |\mathbf{k}_T|}, \quad (5)$$

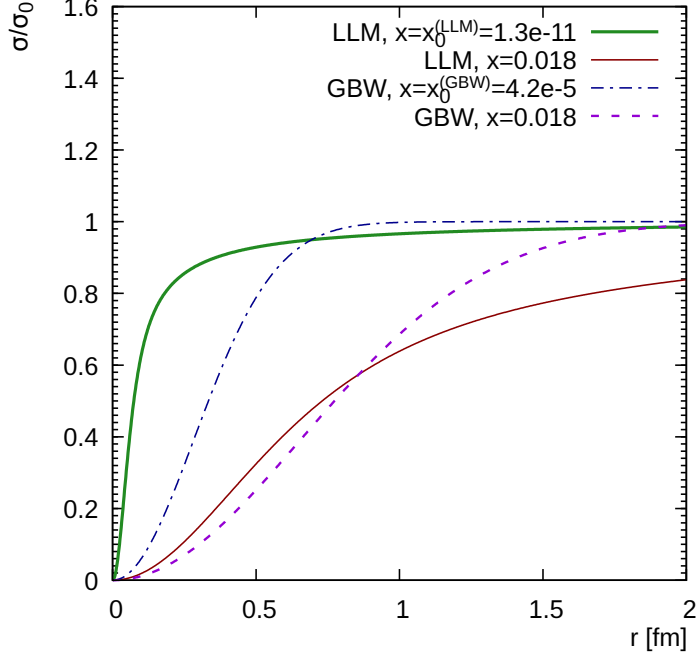


Рис. 1. The effective dipole cross section $\hat{\sigma}(x, r^2)$ normalized by σ_0 calculated as a function of r at different values of x .

where $R_0(x)$ is defined in (4) and we kept $x_0 = 4.1 \cdot 10^{-5}$ and $\lambda = 0.22$. Our best fit for phenomenological parameters leads to $c_1 = 5$, $c_2 = 3$, $c_3 = 2$ and $Q_0 = 1.233$ GeV.

We treat b_g as a running parameter at $\mathbf{k}_T^2 \geq Q_0^2$:

$$b_g = b_g(0) + \frac{4C_A}{\beta_0} \ln \frac{\alpha_s(Q_0^2)}{\alpha_s(\mathbf{k}_T^2)}, \quad (6)$$

where $b_g(0) = 5.854$, $C_A = N_c$ and $\beta_0 = 11 - 2/3N_f$ is the first coefficient of the QCD β -function. At small $\mathbf{k}_T^2 < Q_0^2$, the fixed value $b_g = b_g(0)$ is used.

The relation of the cross section of the virtual photon γ^* with proton is presented in [6, 7] calculated within the two-gluon exchange approximation and has the following form:

$$\hat{\sigma}(x, r^2) = \frac{4\pi^2\alpha_s}{3} \int \frac{d\mathbf{k}_T^2}{\mathbf{k}_T^2} \{1 - J_0(|\mathbf{k}_T|r)\} f_g(x, \mathbf{k}_T^2), \quad (7)$$

where J_0 is the Bessel function of zero order and $\alpha_s = 0.2$. In Fig 1 the cross section $\hat{\sigma}(x, r^2)$ is presented for the starting gluon TMDs LLM-2022 and GBW. In Fig. 1 we plot the effective dipole cross section $\hat{\sigma}(x, r^2)$ evaluated according to (7) as a function of r at different values of x . We find that its saturation dynamics at large r strongly depends on x and TMD gluon density in a proton. In accordance with (??), the GBW gluon density results in the saturation in the region of $r_s \sim 2/R_0$ (see also discussion [7]). The

corresponding saturation scale at $x = x_0 = 4.2 \cdot 10^{-5}$ and $Q_0 = 1$ GeV is $Q_s \simeq 2/r_s \simeq 0.8$ GeV. The LLM gluon TMD results in approximately the same Q_s at fitted $x_0 = 1.3 \cdot 10^{-11}$ and $Q_0 = 2.2$ GeV, see Fig. 1. The effective dipole cross section, $\sigma^{\gamma^*p}(x, Q^2)$ and gluon density $f_g(x, \mathbf{k}_T^2)$ should not depend on Q^2 at low $Q^2 < Q_s^2$.

With the listed pocket formulas we can now calculate some observables. The structure function F_2 is the sum of the transverse structure function F_T and longitudinal one F_L , i.e.,

$$F_2(x, Q^2) = F_T(x, Q^2) + F_L(x, Q^2). \quad (8)$$

F_T and F_L can be calculated at low x neglecting small term mx^2 using (??):

$$F_{T,L}(x, Q^2) = \frac{Q^2}{4\pi^2\alpha_{em}}\sigma_{T,L}(x, Q^2), \quad (9)$$

In fact, the reduced cross section σ_r in the $e p$ DIS, which is related to structure functions F_2 and F_L , is measured; it can be calculated as:

$$\sigma_r = \frac{Q^4 x}{2\pi\alpha^2(1-y^2)} \frac{d^2\sigma}{dx dQ^2} = F_2(x, Q^2) - f(y)F_L(x, Q^2), \quad (10)$$

where $d^2\sigma/dxdQ^2$ is the double differential DIS cross section, $f(y) = y^2/(1 + (1-y)^2)$ with inelasticity $y = Q^2/(sx)$ and $s = 4E_e E_p$, E_e and E_p are the electron and the proton energies respectively. Having determined the parameters we can now easily calculate the structure function $F_2(x, Q^2)$. We show our results in comparison with low Q^2 ZEUS [15] and H1 [14] data in Fig. 3. A good agreement of LLM results with data is achieved.

3. Soft pp processes at LHC energies and mid-rapidity

Now we turn to the production of soft charged hadrons in pp collisions at the LHC energies. These processes are very sensitive to the gluon density in a proton at low scales $\mu \sim p_T \simeq 1$ GeV. In the calculations we employ the modified QGSM, see [16, 17] and references therein, and strictly follow the approach described earlier [3]. So, the inclusive hadron spectrum at low p_T and mid-rapidities splits into two pieces: the quark contribution ρ_q and the gluon one ρ_g :

$$\rho(x, p_T) = E \frac{d^3\sigma}{d^3p} \equiv \frac{1}{\pi} \frac{d^3\sigma}{d^2p_T dy} = \rho_q(x, p_T) + \rho_g(x, p_T). \quad (11)$$

First term is calculated within the conventional QGSM using only one-Pomeron exchange. It can be done because in the mid-rapidity and small $x_T = 2p_T/\sqrt{s}$ the multi-Pomeron exchanges give negligibly small contributions [18]. The second one, $\rho_g(x, p_T)$, is calculated as a convolution of the "modified" gluon distribution with fragmentation function (FF) of gluons

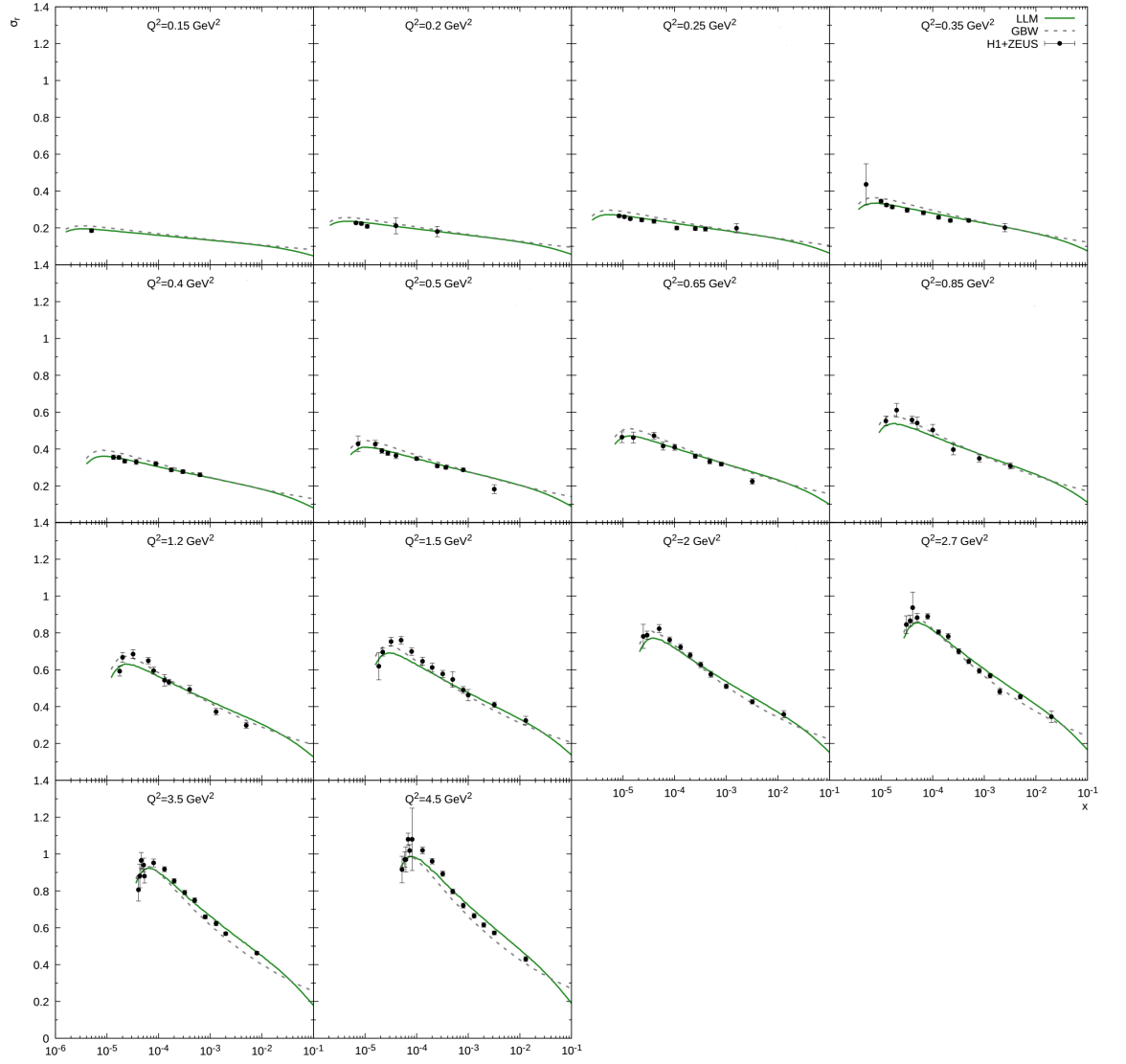


Рис. 2. The reduced DIS cross section a function of x at different Q^2 at $\sqrt{s} = 318$ GeV. The solid line corresponds to the gluon TMD of type LLM [3], the dashed line is the calculation with GBW gluon TMD [6, 7]. The data are taken from ZEUS and H1 [12–15].

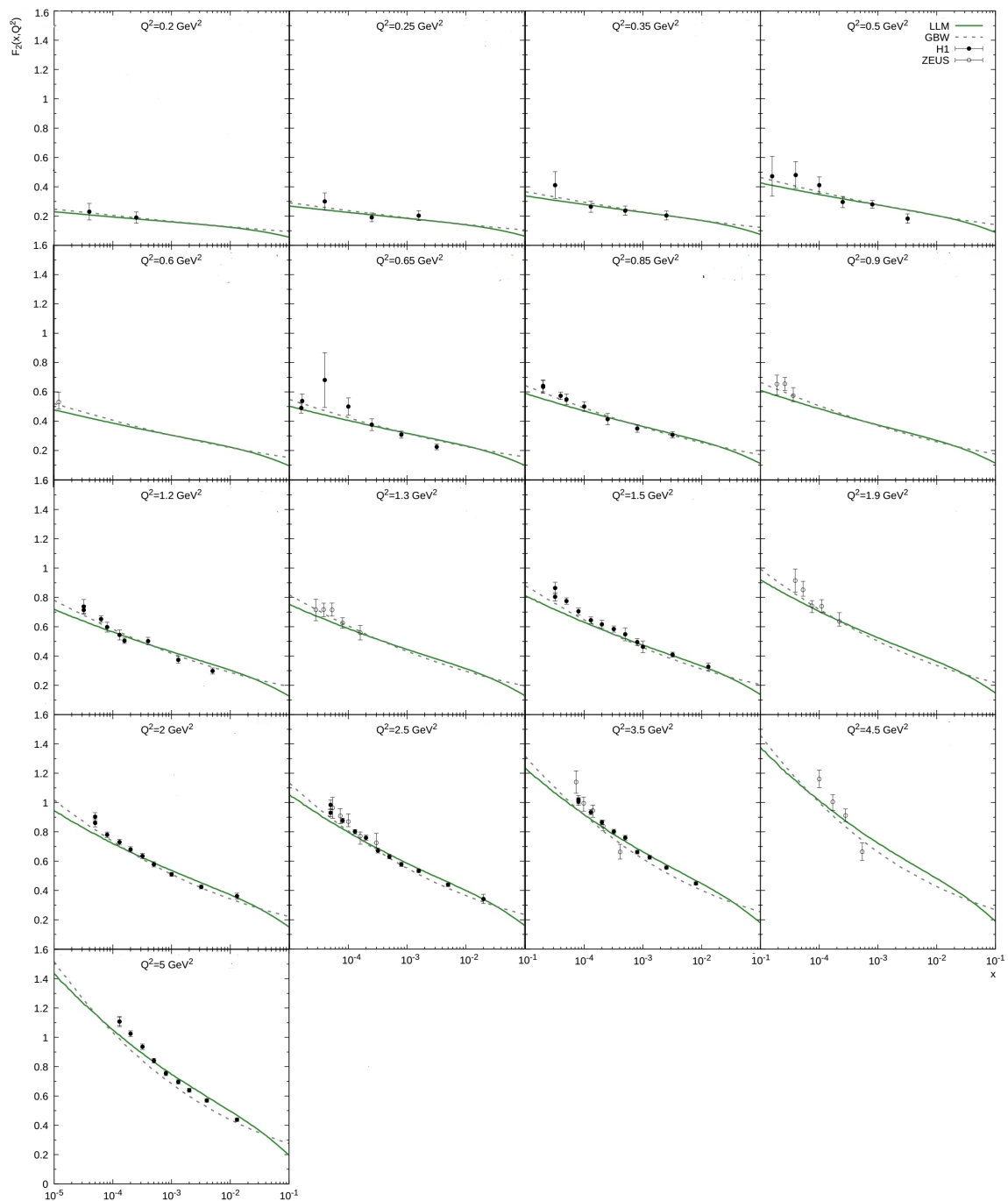


Рис. 3. The structure function F_2 as a function of x at different Q^2 . The notations of the lines are the same as on Fig. 2. The data are taken from ZEUS [12, 13, 15] (white circles) and H1 [14] (black circles).

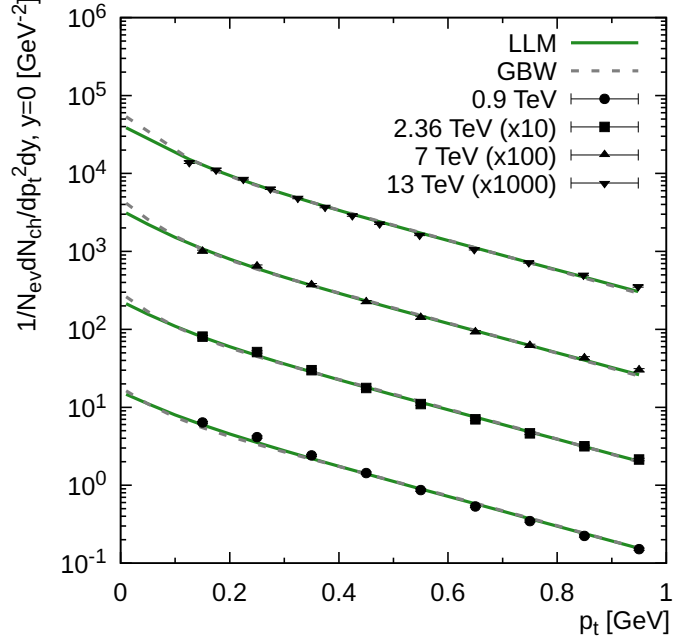


Рис. 4. Transverse momentum distributions of soft charged hadrons produced in pp collisions at different LHC energies in the mid-rapidity region. The notations of the lines are the same as in Fig. 3. The experimental data are from [20–22].

into hadrons $G_{g \rightarrow h}(z, |\tilde{\mathbf{p}}_T|)$ multiplied by the inelastic pp cross section (see, for example, [3] for more details). These FFs were calculated at leading (LO) and next-to-leading (NLO) orders [19] and presented in a factorized form $G_{g \rightarrow h}(z, |\tilde{\mathbf{p}}_T|) = G_{g \rightarrow h}(z) I_h^g(|\tilde{\mathbf{p}}_T|)$, where $I_h^g(|\tilde{\mathbf{p}}_T|)$ could be approximated as:

$$I_h^g(|\tilde{\mathbf{p}}_T|) = \frac{B_h^g}{2\pi} \exp(-B_h^g |\tilde{\mathbf{p}}_T|). \quad (12)$$

Here $\tilde{p}_T = p_T - zk_T$ with p_T and k_T being the transverse momenta of the produced hadron h and gluon, respectively. The FFs of quarks and/or diquarks into hadrons h can be expressed in a similar way. Below we repeat the calculations [3] with the LLM gluon density and newly fitted values of x_0 , λ and $Q_0 = 2.2$ GeV. We find that the best description of the LHC data collected at different energies ($\sqrt{s} = 0.9, 2.36, 7$ and 13 TeV) is achieved with slope parameters $B_h^g = 4.35$ GeV $^{-1}$, $B_h^q = B_h^{qq} = 5.42$ GeV $^{-1}$ ($\chi^2/n.d.f. = 3.5$). All other parameters involved into the calculations and listed in [3] are unchanged. Our results are shown in Fig. 4. One can see that good agreement with the measurements is obtained in a wide range of energies. For a comparison we also show results obtained with the GBW TMD. It results in a different fit of the fragmentation parameters $B_h^g = 4.75$ GeV $^{-1}$, $B_h^q = B_h^{qq} = 6.5$ GeV $^{-1}$, which, however, gives a worse description ($\chi^2/n.d.f. = 5.9$).

The investigation of strange hadron and pion production in heavy-ion collisions is a promising tool to search for new physical properties of such processes. The observation of a sharp peak in the production ratio of K^+ mesons to π^+ mesons in central $PbPb$ and $AuAu$ collisions at mid-rapidity [?, ?] has attracted the attention of both theoreticians and experimentalists, see [3-25] and references therein. When the initial energy $\sqrt{s_{NN}}$ per nucleon becomes larger than 30 GeV this ratio falls down. According to the suggestion of [23, 24] this peak (so-called ‘‘horn’’) can be due to formation of a quark-gluon plasma (QGP) phase at the center-of-mass energy $\sqrt{s} \simeq 7$ GeV. There are another models explaining a reason of this ‘‘horn’’, see [25] and referencies therein. However, the ratio of K^+ to π^+ mesons produced in collisions of nuclei lighter than Pb and Au , as a function of the initial energy $\sqrt{s_{NN}}$, in particular, $BeBe$ [26] and $ArSc$ [27] has no peak, as revealed by the NA61/SHINE Collaboration [26, 27]. The fast increase of this ratio, when $\sqrt{s_{NN}}$ grows from the kaon threshold up to 20-30 GeV and the slow increase at larger energies have been observed [26, 28]. Moreover, the energy dependence of K/π ratios observed in $BeBe$ collisions [26] is similar to the one in pp collisions.

In this paper we analyze the production of kaons and pions in $BeBe$ collisions at mid-rapidity and focus on ratios between their cross-sections as functions of the initial energy within the same theoretical approach, which was presented in [30] for pp collisions. This approach is based on the similarity of the inclusive hadron spectra produced in AA collisions at mid-rapidity satisfied to the conservation laws of four-momenta and quantum numbers [30–34].

The inclusive production of hadron 1 in the interaction of nucleus A with nucleus B

$$A + B \rightarrow 1 + \dots, \quad (13)$$

is satisfied by the conservation law of four-momenta in the following form [33, 34]

$$(N_A P_A + N_B P_B - p_1)^2 = (N_A m_0 + N_B m_0 + M)^2, \quad (14)$$

where N_A and N_B are the fractions of the four-momentum transmitted by nucleus A and nucleus B , the forms of N_A, N_B are presented in [34]; P_A, P_B, p_1 are the four-momenta of nuclei A, B and particle 1, respectively; m_0 is the mass of the nucleon; M is the mass of the particle providing for conservation of the baryon number, strangeness and other quantum numbers. Eq. 14 was introduced in [33, 34] for the production of hadrons in AB collisions in the kinematics forbidden for free nucleon-nucleon collisions. In fact, it is valid for initial energies of colliding nuclei close to the threshold of hadron production. It allows us to find the minimal value of M , which provides for the conservation of quantum numbers. For π -mesons $m_1 = m_\pi$ and $M = 0$. For antinuclei $M = m_1$ and for K^- -mesons $M = m_1 = m_K$, m_K is the mass of the K -meson. For nuclear fragments $M = -m_1$. For K^+ -mesons $m_1 = m_K$ and $M = m_\Lambda - m_0$, m_Λ is the mass of the Λ -baryon. Let us note that the isospin effects of the produced hadrons and other nuclear effects are

out of this approach. Therefore, it is assumed that within the self-similarity approach there is no big difference between the inclusive spectra of π^+ and π^- mesons produced in pp and AA collisions. However, there is a difference between similar spectra of K^+ and K^- mesons, because the values of M are different. This is due to the conservation law of strangeness.

In [33, 34] the parameter of self-similarity is introduced in the following form

$$\Pi = \min \frac{1}{2} [(u_A N_A + u_B N_B)^2]^{1/2}, \quad (15)$$

where u_A and u_B are the four-velocities of nuclei A and B , respectively. The minimization over N presented in Eq. (15) allows us to find the parameter Π . This parameter introduced in [33] was obtained as the analytical form in [34] for nucleus-nucleus collisions in the mid-rapidity region, however, it can also be applied successfully for the analysis of pion production in pp collisions.

The inclusive spectrum of particle 1 produced in the AB collision can be parametrized as a general universal function dependent on the self-similarity parameter Π , as it was shown in [36].

$$E d^3 \sigma_{AB} / d^3 p = A_A^{\alpha(N_A)} \cdot A_B^{\alpha(N_B)} \cdot F(\Pi) \quad (16)$$

where $\alpha(N_A) = 1/3 + N_A/3$, $\alpha(N_B) = 1/3 + N_B/3$ and function $F(\Pi)$ is the inclusive spectrum of hadron production in the AB collision [35].

For symmetric colliding nuclei $N_A = N_B = N$ the function Π is found from the minimization of Eq. 15 by solving the equation. This assumption has been suggested in [33, 34]

$$\frac{d\Pi}{dN} = 0 \quad (17)$$

The exact solution of Eq. 17 at $y = 0$, as

$$N = \frac{\Pi}{\cosh(Y)} \equiv \frac{2m_0\Pi}{\sqrt{s}}, \quad (18)$$

was obtained in [33, 34], for details see, also [35]. In Eq. 18 Y is rapidity of colliding nuclei. Therefore, $\alpha(N) = 1/3 + 2m_0\Pi/(3\sqrt{s})$. For symmetric nuclei Eq. 16 is presented in the following form

$$E d^3 \sigma_{AA} / d^3 p = A^{2\alpha(N)} \cdot F(\Pi) \quad (19)$$

$$F(\Pi) = \left[A_q \exp\left(-\frac{\Pi}{C_q}\right) + A_g \sqrt{p_T} \phi_1(s) \exp\left(-\frac{\Pi}{C_g}\right) \right] \sigma_{tot} \quad (20)$$

where

$$\Pi(s, m_{1T}, y) = \left\{ \frac{m_{1T}}{2m_0\delta_h} + \frac{M}{\sqrt{s}\delta_h} \right\} \cosh(y)G, \quad (21)$$

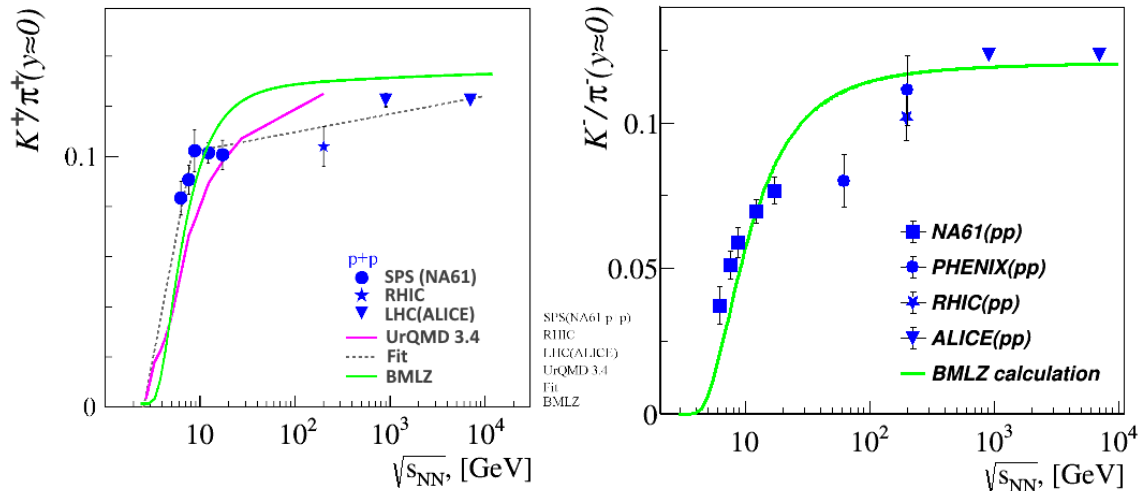


Рис. 5. Left: the ratio of cross sections $\sigma_{K^+}/\sigma_{\pi^+}$ in pp collisions as a function of \sqrt{s} . Right: the similar ratio for $\sigma_{K^-}/\sigma_{\pi^-}$.

$$G = \left\{ 1 + \sqrt{1 + \frac{M^2 - m_1^2}{(m_{1T} + 2Mm_0/\sqrt{s})^2 \cosh^2(y)} \delta_h} \right\} \dots \quad (22)$$

Here $\phi_1(s) = 1 - \sigma_{nd}(s)/\sigma_{tot}(s)$, see [35],

$\delta_h = \left(1 - \frac{s_{th}^h}{s}\right)$; $s_{th}^\pi \simeq 4m_0^2$; $s_{th}^{K^+} = (m_0 + m_K + m_\Lambda)^2$; $s_{th}^{K^-} = (2m_0 + 2m_K)^2$; $M = m_\Lambda - m_0$; $m_\Lambda = 1.115$ GeV; $m_K = 0.494$ GeV; $s_0 = 1$ GeV; $m_0 = 0.938$ GeV; p_{1T} and m_{1T} are the transverse momentum and transverse mass of the produced hadron 1; $\sigma_{nd} = (\sigma_{tot} - \sigma_{el} - \sigma_{SD})$ is the non-diffractive cross-section; σ_{tot} , σ_{SD} and σ_{el} are the total cross-section, the single diffractive cross-section and the elastic cross-section of pp collisions, respectively.

5. Summary

Suggested gluon TMD at low Q^2 is applied successfully to the analysis of the ep DIS, pp and AA collisions at high and middle energies and mid-rapidity. Note that the form for $F(\pi)$ in Eq. 21 was suggested first in [18] for best description of charge hadrons produced in pp collisions at LC energies and low transverse momenta in the mid-rapidity region assuming the creation of nonperturbative gluons at low Q^2 and their transverse momenta k_T . In the latest our papers [3,4] these gluon distributions were related to the saturation effect in the ep DIS mentioned in Sect.2.

Acknowledgements. We thank S.P. Baranov, H. Jung, S. Schmidt and S. Taheri Monfared for their interest, important comments and remarks. Establishing new TMD and fragmentation functions parameters as well as soft hadron production simulations and the dipole cross sections calculations were supported by the Russian Science Foundation under grant 22-22-00387. The

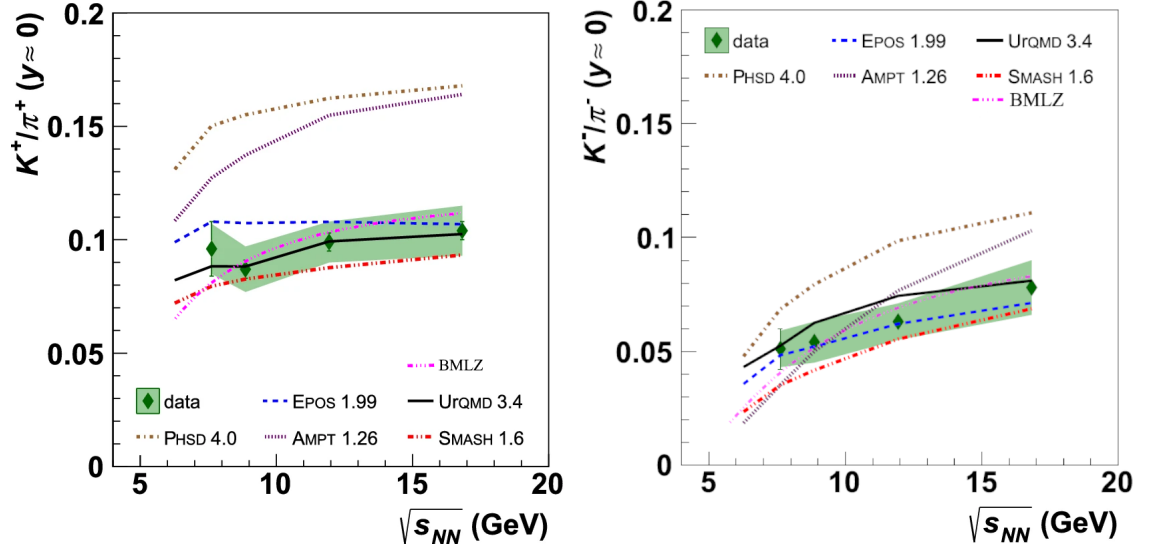


Рис. 6. Left: the ratio of cross sections $\sigma_{K^+}/\sigma_{\pi^+}$ in $BeBe$ collisions as a function of \sqrt{s} . Right: the similar ratio for $\sigma_{K^-}/\sigma_{\pi^-}$.

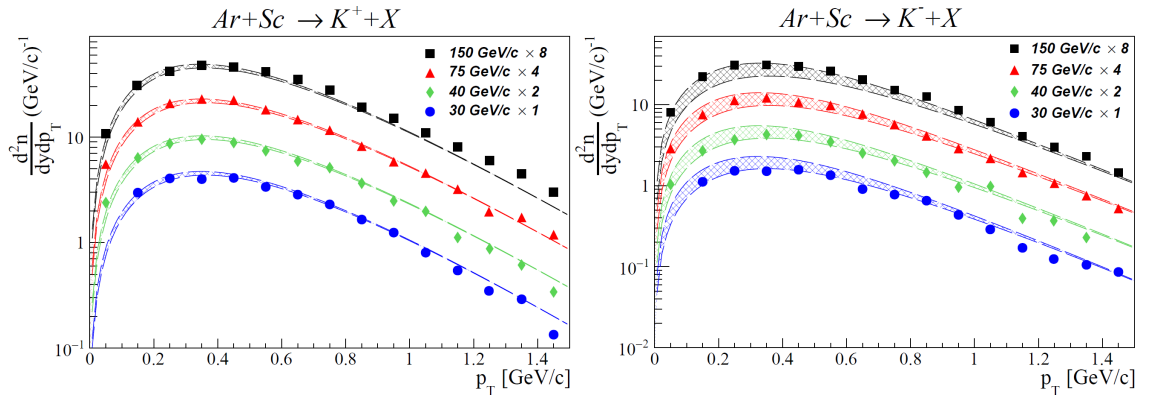


Рис. 7. Left: inclusive p_T -spectra of K^+ -mesons produced in $ArSc$ collisions at mid-rapidity ($y \approx 0$) and different initial energies $\sqrt{s_{NN}}$. Right: the similar p_T -spectra but for K^- -mesons.

reduced cross section and structure function calculation and corresponding TMD refitting was performed with support of Russian Science Foundation under grant 22-22-00119.

СПИСОК ЛИТЕРАТУРЫ

1. V.N. Gribov, L.N. Lipatov, Sov. J. Nucl. Phys. **15**, 438 (1972);
L.N. Lipatov, Sov. J. Nucl. Phys. **20**, 94 (1975);
G. Altarelli, G. Parisi, Nucl. Phys. B **126**, 298 (1977);
Yu.L. Dokshitzer, Sov. Phys. JETP **46**, 641 (1977).
2. M. Ciafaloni, Nucl. Phys. B **296**, 49 (1988);
S. Catani, F. Fiorani, G. Marchesini, Phys. Lett. B **234**, 339 (1990);
S. Catani, F. Fiorani, G. Marchesini, Nucl. Phys. B **336**, 18 (1990);
G. Marchesini, Nucl. Phys. B **445**, 49 (1995).
3. A.V. Lipatov, G.I. Lykasov, M.A. Malyshev, Phys.Rev. D **107**, 014022 (2023).
4. A.V. Lipatov, G.I. Lykasov, M.A. Malyshev, Phys.Lett.B **839**, 137780 (2023).
5. F. Hautmann and H. Jung, Nucl.Phys. B**883** (2014).
6. K. Golec-Biernat, M. Wuesthoff, Phys.Rev.D **59**, 014017 (1998).
7. K. Golec-Biernat, M. Wuesthoff, Phys.Rev.D **60**, 114023 (1999).
8. L.V. Gribov, E.M. Levin, M.G. Ryskin, Phys. Rep. **100**, 1 (1983)
9. A.H. Mueller, Nucl.Phys., B **335**, 115 (1990).
10. N. Nikolaev, E.P. Predazzi, B.G. Zakharov, Phys. Lett. B**326**, 161 (1994).
11. N. Nikolaev, B.G. Zakharov, Z.Phys. C**49**, 607 (1990).
12. ZEUS Collaboration, Phys.Lett., B**487**, 53 (2000).
13. ZEUS Collaboration, Eur.Phys. J. C **21**, 443 (2001).
14. H1 Collaboration, Eur.Phys.J. C **63**, 625 (2009), arXiv:0904.0929 [hep-ph].
15. ZEUS Collaboration, Eur.Phys. J. C **7**, 609 (1998).
16. A.B.Kaidalov, Z.Phys., **C12**, 63 (1982); Sarveys High Energy Phys., **13**, 265 (1999). A.B.Kaidalov, O.I.Piskunova, Z.Phys., C**30**, 145 (1986); Yad.Fiz., **43**, 1545 (1986).
17. G.I.Lykasov, G.G.Arakelyan, M.N.Sergeenko, EPAN,v.30,p.817 (1999).

18. V.A. Bednyakov, A.A. Grinyuk, G.I. Lykasov, M. Poghosyan, *Int.J.Mod.Phys., A* **27**, 125042 (2012).
19. J.Binnewies, B.A. Kniehel, G. Kramer, *Phys.Rev. D* **52**, 4947 (1995).
K.A.Ter-Martitosyan, *Sov.J. Nucl.Phys.*,**44**, 817 (1986).
20. CMS Collaboration, *Phys.Rev.Lett.*, **105**, 022002 (2010).
21. ATLAS Collaboration., *New J.Phys.* **13**, 053033 (2011)
22. ATLAS Collaboration., *Eur.Phys.J C***76**, 502 (2016).
23. M. Gazdzicki, M.I. Gorenstein, *Acta Physika Polon.*, B **30**, 2705 (1999).
24. M. Gazdzicki, M.I. Gorenstein, P. Seyboth, *J.Mod.Phys. E* **23**, 1430008 (2014).
25. G.I. Lykasov, A.I. Malakhov, A.A. Zaitsev, *Eur. Phys. J. A* **58** , 112 (2022)
26. A. Acharya, et al., (NA61/SHINE Collaboration) *Eur. Phys. j. C* **81**, 73 (2021).
27. Maja Mackowiak-Pawłowska for the NA61/SHINE Collaboration, [arXiv:2112.01877 \[nucl-ex\]](https://arxiv.org/abs/2112.01877).
28. A. Acharya *et al.*, (NA61/SHINE Collaboration), *Eur. Phys. J. C* **81**, 397 (2021)
29. A. Aduszkiewicz, et al., (NA61/SHINE Collaboration) *Phys.Rev.C* **102**, 011901(R) (2020).
30. G.I. Lykasov, A.I. Malakhov, A.A. Zaitsev, *Eur. Phys. J. A* **57** , 78 (2021).
31. A.M. Baldin, L.A. Didenko, *Fortsch.Phys.* **38**, 261 (1990).
32. A. M.Baldin, A. A. Baldin. *Phys. Particles and Nuclei*, **29** No3, 232 (1998).
33. A.M. Baldin, A.I. Malakhov, and A. N. Sissakian, *Phys. Part. Nucl.* **29** (Suppl. 1), 4 (2001).
34. A.M. Baldin, A.I. Malakhov. *JINR Rapid Communications*, No.1(87)-98, pp.5-12 (1998).
35. G.I. Lykasov, A.I. Malakhov, *Eur. Phys. J. A* **56**, 187 (2018).
36. Baldin A.A. *JINR Rapid Comm.* No. 4[78]-96 p.61-68.